Role of *luxS* in *Bacillus anthracis* growth and virulence factor expression

Marcus B. Jones, Scott N. Peterson, Rosslyn Benn, John C. Braisted, Behnam Jarrahi, Kenneth Shatzkes, Dacheng Ren, Thomas K. Wood & Martin J. Blaser

Role of *luxS* in *Bacillus anthracis* growth and virulence factor expression

Marcus B. Jones,[1-3,*] Scott N. Peterson,[1] Rosslyn Benn,[1] John C. Braisted,[1] Behnam Jarrahi,[1] Kenneth Shatzkes,[1] Dacheng Ren,[4] Thomas K. Wood[5] and Martin J. Blaser[2,3]

[1]Pathogen Functional Genomics Resource Center (PFGRC); J. Craig Venter Institute (JCVI); Rockville, MD USA; [2]Department of Medicine; New York University School of Medicine; New York, NY USA; [3]Department of Microbiology; Sackler Institute; New York University School of Medicine; New York, NY USA; [4]Departments of Biomedical and Chemical Engineering; Civil and Environmental Engineering; and Biology; Syracuse Biomaterials Institute; Syracuse University; NY, USA; [5]Artie McFerrin Department of Chemical Engineering; Texas A&M University; College Station, TX USA

Quorum-sensing (QS), the regulation of bacterial gene expression in response to changes in cell density, involves pathways that synthesize signaling molecules (auto-inducers). The *luxS*/AI-2-mediated QS system has been identified in both Gram-positive and Gram-negative bacteria. *Bacillus anthracis*, the etiological agent of anthrax, possesses genes involved in *luxS*/AI-2-mediated QS, and deletion of *luxS* in *B. anthracis* Sterne strain 34F$_2$ results in inhibition of AI-2 synthesis and a growth defect. In the present study, we created a Δ*luxS B. anthracis* strain complemented in trans by insertion of a cassette, including *luxS* and a gene encoding erythromycin resistance, into the truncated *plcR* regulator locus. The complemented Δ*luxS* strain has restored AI-2 synthesis and wild-type growth. A *B. anthracis* microarray study revealed consistent differential gene expression between the wild-type and Δ*luxS* strain, including downregulation of the *B. anthracis* S-layer protein gene EA1 and pXO1 virulence genes. These data indicate that *B. anthracis* may use *luxS*/AI-2-mediated QS to regulate growth, density-dependent gene expression and virulence factor expression.

Introduction

Bacillus anthracis is a gram-positive, non-motile, rod-shaped bacterium that is the etiological agent of anthrax.[1-3] The virulent nature of *B. anthracis* is attributed to two large plasmids, the 181.6 kb pXO1 and the 96.2 kb pXO2, that encode primary pathogenetic factors, including toxin production and capsule formation, respectively.[4-12] The three proteins that comprise the two *B. anthracis* toxins are lethal factor (LF), edema factor (EF) and protective antigen (PA). In two different combinations, these three proteins comprise the lethal toxin (PA + LF) and the edema toxin (PA + EF).[5,7,9-18] Maximum production of toxins occurs during the transition from log to the stationary phase of growth, suggesting growth phase-regulation of expression.[19]

Quorum-sensing (QS) is a process by which bacteria regulate the expression of density- and growth phase-dependent genes.[20-25] QS involves the synthesis, release and detection of small signaling molecules, termed auto-inducers. The auto-inducer concentration is directly correlated to the bacterial population. Utilization of QS systems is critical for the regulation of virulence gene expression in many pathogenic bacteria. Inhibition of QS circuits by QS antagonists, such as the halogenated furanones from the red-sea alga *Delisea pulchra*, offers an attractive method for inhibiting bacterial pathogens.[26-36]

B. anthracis synthesizes AI-2 or an AI-2-like auto-inducer molecule that induces bioluminescence in the *Vibrio harveyi* bioassay.[37] Furthermore, analysis of the *B. anthracis* genome indicated the presence of a gene, *luxS*, which typically is involved in QS. Disruption of *luxS* resulted in the inability of *B. anthracis* to synthesize a functional AI-2 or AI-2-like molecule recognizable in the *V. harveyi* bioassay, and in a defect in growth in vitro for the *B. anthracis luxS* mutant.[37] These data suggest that *B. anthracis* may utilize the *luxS*/AI-2 QS system to regulate growth as well as density-dependent gene expression.

In the present report, we characterize the differential gene expression of *Bacillus anthracis* strains 34F$_2$, 34F$_2$Δ*luxS* and 34F$_2$*luxS*:comp. To further characterize the role of QS in *B. anthracis*, by microarray analysis we analyzed *B. anthracis* gene expression in wild-type cells grown in the presence or absence of halogenated furanones. Finally we utilize a custom tiled genome Affymetrix array to identify possible small RNAs differentially expressed in the *luxS* mutant compared to the wildtype.

Results

Complementation of AI-2 deficiency. Cell-free medium (CFM) was collected from *B. anthracis* strains 34F$_2$, 34F$_2$:Δ*luxS* and 34F$_2$Δ*luxS*:comp for assessment in the *Vibrio harveyi* BB170 bioluminescence assay. The AI-2 bioassay utilizes a deficiency in the AI-1 sensor in *V. harveyi* strain BB170. Without the *luxN* AI-1 encoded sensor, strain BB170 only exhibits bioluminescence in response to AI-2 or an AI-2-like molecule. Growth of strain
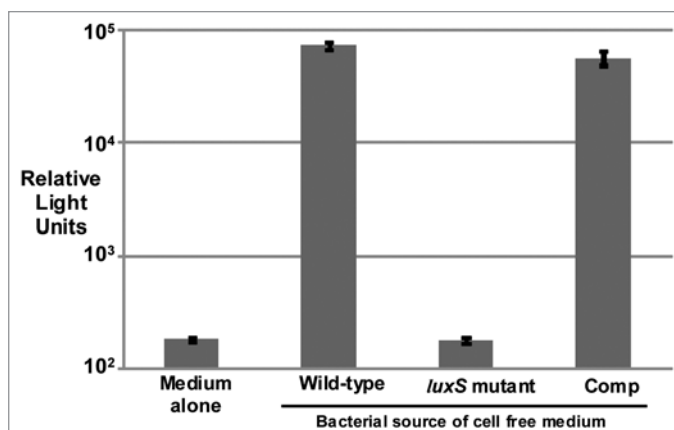
Figure 1. Induction of bioluminescence in *V. harveyi* reporter strain by CFM from *B. anthracis* cells. *V. harveyi* strain BB170 only upregulates the expression of the *lux* operon [measured as relative light units (RLU)], when AI-2 or AI-2-like molecules are present in its milieu. Cell free medium (CFM) obtained from AI-2-synthesizing bacteria can induce expression of the bioluminescence-generating *luxCDABE* operon in BB170. (A) In the experiments shown, CFM from 5-h cultures of *B. anthracis* strains $34F_2$ and $34F_2\Delta luxS$ and sterile CFM alone were used as positive and negative controls. The baseline is the value when uninoculated (sterile) CFM alone at 5 h were used. Each bar represents the mean (±SD) of triplicate experiments. Compared to the negative and positive controls, $34F_2\Delta luxS:comp$ showed restored AI-2 activity compared to wild-type $34F_2$. (B) In the experiment shown, CFM from 5-h cultures of wild-type $34F_2$ and $34F_2\Delta luxS:comp$ were serially diluted 1:1, 1:10 and 1:100. Each bar represents the mean (±SD) of triplicate experiments.

BB170 overnight, followed by dilution 1:10,000 (to yield low cell density), reduces the level of endogenous AI-2 below the threshold required for luminescence. In this experimental system, the addition of exogenous AI-2 from bacteria possessing *luxS* function can restore the bioluminescence phenotype of the BB170 cells. As a negative control, the *V. harveyi* reporter strain BB170 was incubated with sterile cell-free medium (CFM) alone, and as a positive control, CFM from a high-density culture of strain BB170 was used (**Fig. 1**). Addition of sterile CFM to cells of BB170 served as the standard for baseline luminescence, whereas, as expected, addition of CFM from the high-density BB170 culture induced a >100-fold increase in luminescence. Additional controls included were CFM from *B. anthracis* strain $34F_2\Delta luxS$ (negative control) and *B. anthracis* $34F_2$ (positive control). CFM from *B. anthracis* strain $34F_2\Delta luxS$:comp exhibits AI-2 activity comparable to that of the wild-type strain (**Fig. 1**). These data demonstrate that the *luxS* chromosomal complementation fully restored AI-2 production that was deficient in *B. anthracis* strain $34F_2\Delta luxS$ (**Fig. 1**).

Complementation of the growth defect in *B. anthracis* strain $34F_2\Delta luxS$. When cultured in liquid medium, *B. anthracis* $34F_2\Delta luxS$ exhibited a moderate, but reproducible, growth defect compared to wild-type *B. anthracis* $34F_2$.[37] To determine whether the growth defect was directly related to the deletion of *luxS*, we compared the growth of *B. anthracis* wild-type strain $34F_2$, strain $34F_2\Delta luxS$, and the $34F_2\Delta luxS$:comp strain. As determined by triplicate cell densities and based on OD_{600}, the $34F_2\Delta luxS$:comp strain showed restored growth compared to the

$\Delta luxS$ strain (**Fig. 2**). These data suggest that *luxS*/AI-2-mediated quorum sensing is involved in regulating metabolic functions in *B. anthracis* under aerobic conditions. Based on these findings, we sought to characterize the growth defect in $34F_2\Delta luxS$ by examining the transcriptional profile of the $34F_2\Delta luxS$ strain compared to the wild type parental strain.[37]

Differential gene expression of a *B. anthracis* $34F_2\Delta luxS$ strain grown aerobically. To identify genes regulated by the *luxS/AI-2* QS system, *B. anthracis* microarrays were utilized. Total RNA was isolated from *B. anthracis* strains $34F_2$ and $34F_2\Delta luxS$ grown in BHI in the absence of sodium bicarbonate. Isolated RNA samples were hybridized to spotted *B. anthracis* array slides and analyzed using TM4 software (www.tm4. org).[38] Significance of microarray (SAM) analysis of array data revealed that 576 genes were differentially expressed in the $34F_2\Delta luxS$ strain, compared to the wild-type $34F_2$ strain based on a false discovery cutoff of 7%. Select upregulated genes ≥2-fold (**Table 2**) and downregulated genes ≥2-fold (**Table 3**) are listed. Genes that were not downregulated ≥2-fold, but are in the middle of a presumed operon in which other genes have a ≥2-fold change are included. Among the genes downregulated in the $34F_2\Delta luxS$ strain are the *luxS* gene (as expected), the S-layer virulence gene EA1, encoding putative S-layer proteins, and genes involved in phosphotransferase systems (PTS) (**Table 3**). Genes that were upregulated ≥2-fold included those encoding a phospholipase C, a bacitracin protease and resistance protein (**Table 2**). These data suggest that *luxS*/AI-2 is involved in regulating peptide transport and S-layer expression. To further elucidate impact of *luxS*/AI-2 on *B. anthracis* gene expression we performed an analysis of down and upregulated genes to determine cellular and functional roles. Analysis of downregulated genes revealed that a significant portion are involved in energy metabolism (23%) and transport and binding proteins (12.7%), and analysis of upregulated genes revealed a significant portion are involved with cellular processes (18.8%).

Closer examination of genes downregulated in *B. anthracis* $34F_2\Delta luxS$ strain revealed several operons involved in nitrate/nitrite metabolism (**Table 3**) when grown either aerobically or in the presence of sodium bicarbonate. Nitrate reduction has three fundamental roles: (1) utilization as a nitrogen source (nitrate assimilation); (2) maintenance of oxidation-reduction balance (nitrate dissimilation), and (3) utilization as a terminal electron acceptor (nitrate respiration).[39] In-depth analysis of nitrate/nitrite respiration regulation in *B. subtilis* revealed the ability of the bacterium to convert nitrate or nitrite to ammonium when grown aerobically.[40] The conversion of these nitrogen sources to ammonium is catalyzed by assimilatory nitrate and nitrate reductases. Mutation in *nasD*, *nasE* or *nasF* (assimilatory nitrite reductases) led to growth defects in *B. subtilis* when glucose was depleted.[40] These observations coupled with the transcriptional profile of the $34F_2\Delta luxS$ strain, suggests that *luxS*/AI-2 may play a role in regulating nitrate/nitrite metabolism in *B. anthracis*, and that the observed growth defect in the *luxS* mutant is due to the inability to utilize nitrate/nitrite. It is interesting to note that complementation of *luxS* in *B. anthracis* strain $34F_2\Delta luxS$ did not fully restore the transcriptional expression of the nitrate/nitrite regulon to wildtype
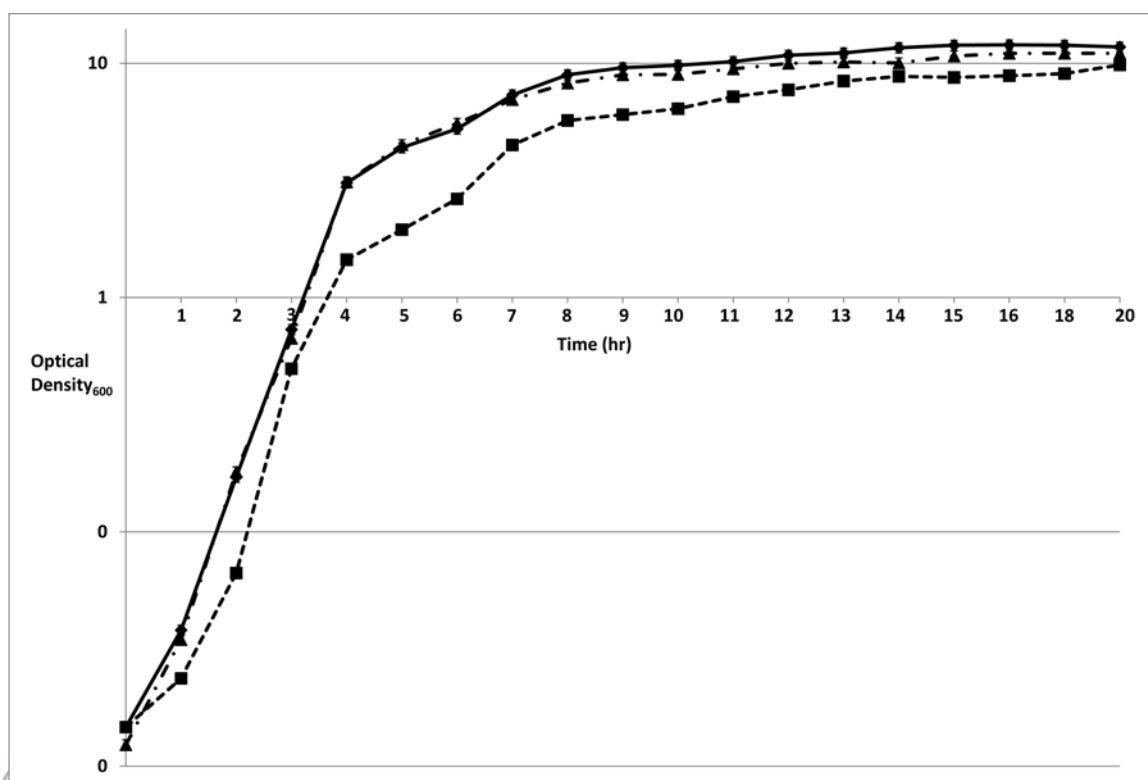
Figure 2. Growth rate analysis of *B. anthracis* 34F$_2$Δ*luxS*:comp. *B. anthracis* strains 34F$_2$, 34F$_2$Δ*luxS*, and 34F$_2$Δ*luxS:comp* were grown overnight and diluted in sterile BHI media to an optical density (OD$_{600}$) of ≈0.01. Cell growth was monitored, CFM removed and passed through a 0.2 μm filter for use in the *V. harveyi* bioassay. The graph represents the mean (±SD) of triplicate experiments performed on the same day. Solid line with filled diamonds represent strain 34F$_2$, dotted line with filled squares represent strain 34F$_2$Δ*luxS* and short dash line with filled triangles represents strain 34F$_2$Δ*luxS*:comp.

(data not shown), suggesting that additional factors may contribute to the growth defect of the *luxS* mutant, and that *luxS*/AI-2 quorum-sensing is not the only factor regulating nitrate/nitrite metabolism. To further elucidate the potential role of *luxS*/AI-2 in nitrate/nitrite metabolism we will make use of inhibitors of AI-2-mediated quorum-sensing.

Differential gene expression of *B. anthracis* 34F$_2$Δ*luxS* grown with 0.8% sodium bicarbonate. QS has been implicated in the regulation of virulence gene expression for a number of pathogenic bacteria.[24,28,30,41-48] To identify genes regulated by the *luxS/AI-2* QS system and CO$_2$/bicarbonate, total RNA was isolated from *B. anthracis* strains 34F$_2$ and 34F$_2$Δ*luxS* grown in BHI in the presence of 0.8% sodium bicarbonate. CO$_2$/bicarbonate is critical for activation of toxin gene expression in *B. anthracis*. Isolated RNA samples were hybridized to spotted *B. anthracis* array slides and analyzed using Spotfinder and TMeV software. Analysis of the microarray data revealed substantial differential expression of virulence genes on plasmid pXO1 in the 34F$_2$Δ*luxS* strain compared to the parental strain 34F$_2$. Genes downregulated on pXO1 include the protective antigen (*pagA*), *pagR*, lethal factor (*lef*) and the calmodulin-sensitive adenylate cyclase (*cya*) (**Table 4, Fig. 3**). **Figure 3** demonstrates temporal changes in gene expression within the pathogenicity island on pXO1 in strain 34F$_2$Δ*luxS* with regard to the downregulation of the toxin components. The virulence regulator *atxA* was only

slightly downregulated in the 34F$_2$Δ*luxS* strain compared to the wild type, suggesting that *luxS*/AI-2 influence on expression of the toxin components is regulated by factors in addition to *atxA*. Analysis of the transcriptional profile of the 34F$_2$Δ*luxS* complement strain revealed near wildtype levels of toxin components *pagA*, *lef* and *cya* compared to the *luxS* mutant strain (**Table 5**). Based on these data, we hypothesize that *luxS*/AI-2 may play a role in influencing additional regulators that modulate toxin expression.

Effect of halogenated furanones on *B. anthracis* gene expression. To better understand the mechanism by which *B. anthracis* may utilize *luxS*/AI-2-mediated QS to regulate gene expression, we studied the effect of halogenated furanones in microarray experiments. Previous studies showed that halogenated furanones can inhibit AI-2-regulated genes in *E. coli* without inhibiting bacterial growth. However, our recent data showed that halogenated furanones inhibit *B. anthracis* growth in a dose-dependent manner.[30] *B. anthracis* cultures were grown to mid-log phase and then supplemented with diluent alone (negative control) or diluent with 20 μg/ml of fur-2.[30] This concentration of fur-2 was selected due to its ability to inhibit expression of *B. anthracis* toxin gene promoter: *lacZ* fusions, and because fur-2 showed no significant toxicity to human THP-1 monocytes at concentrations ≤20 μg/ml (unpublished data). The data reveal that fur-2 can stimulate or inhibit *B. anthracis* gene expression
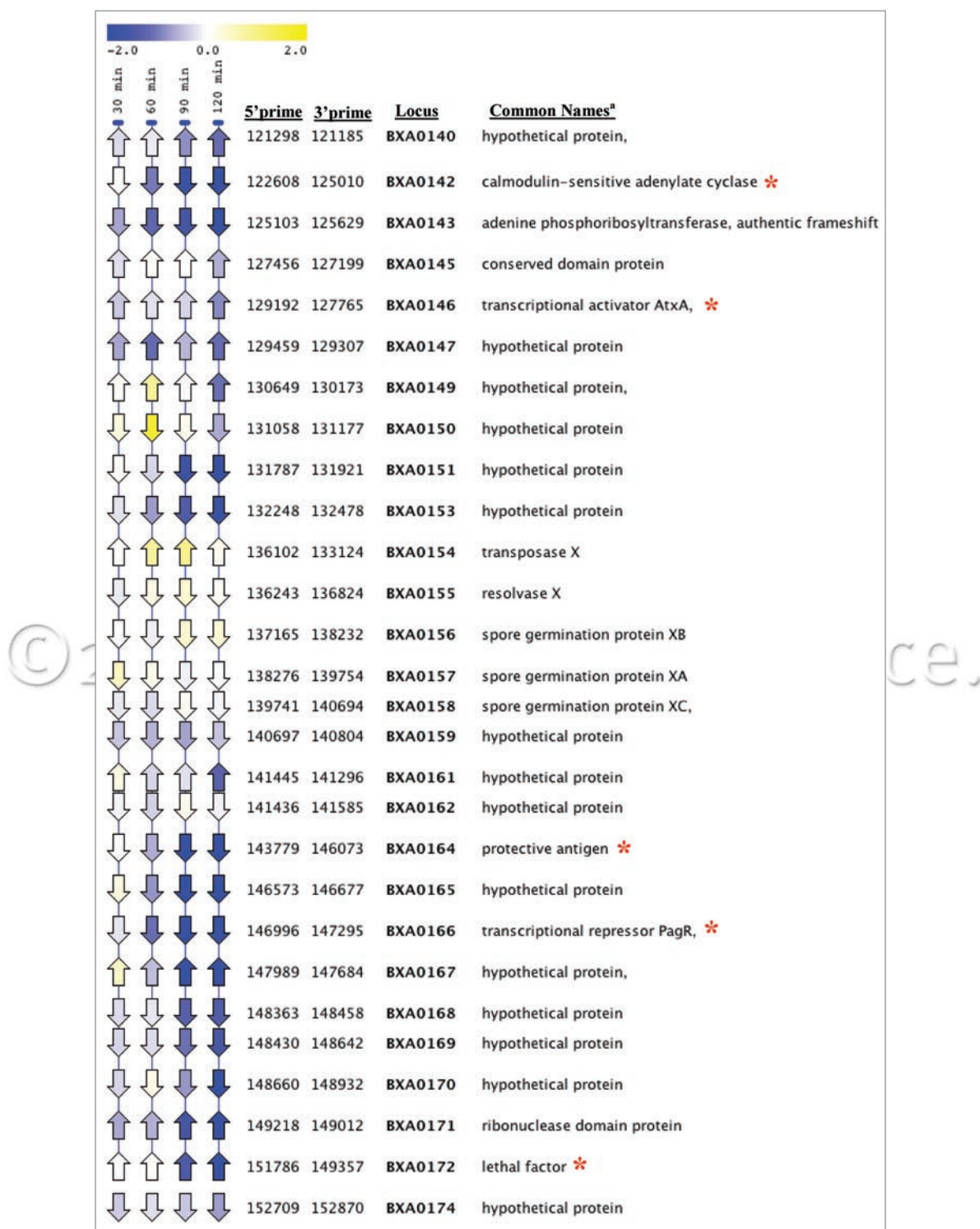
Figure 3. Analysis of pXO1 pathogenicity island gene expression in *B. anthracis* strain 34F₂Δ*luxS* compared to strain 34F₂ using Linear Expression Map (LEM) viewer. Time points are indicated at the top of each column. Arrows indicate the direction of gene orientation. The color scale indicates the log₂ changes in expression, according to the scale shown above. Locus ID based on *B. anthracis* Florida strain A2012. ᵃGenes bolded relate to production or regulation of toxins. ᵇRed asterisk indicates virulence genes.

(Fig. 4). Inhibition and stimulation by fur-2 was not a global event, with only ~5% of the genome showing ≥3-fold differential expression. Expression of the *B. anthracis* toxin components (*lef and pagA*) on pXO1 were significantly downregulated two hours post-exposure to fur-2 (**Table 6**). These data are consistent with the observation that fur-2 significantly inhibits expression of *lacZ* fusions to the promoters of the toxin components.[30] In addition to the toxin components, furanone treatment of *B. anthracis* cells

inhibited respiratory nitrate systems as mentioned above.

To determine whether fur-2 was inhibiting genes regulated by the *luxS*/AI-2 QS system, the differentially expressed genes in cells treated with fur-2 were compared to those differentially expressed in the *B. anthracis* Δ*luxS* strain (**Tables 2 and 3**). Analysis of microarray data revealed that *B. anthracis* toxin components and respiratory nitrate reductase systems were downregulated under both experimental conditions (**Fig. 4**). However, fur-2 did not inhibit the expression of *luxS* directly. These data indicate that fur-2 does not directly inhibit the transcriptional activity of *luxS*, but may interact with the *luxS* product at the cellular level. Furthermore, fur-2 inhibits genes that may be regulated by *luxS*/AI-2 mediated QS in *B. anthracis*. These data support the hypothesis that *luxS*/AI-2-mediated QS may play a role in the regulation of the *B. anthracis* toxin components (*pagA*, *lef* and *cya*) and nitrate/nitrite metabolism.

Analysis of small RNAs in *B. anthracis* 34F$_2$Δ*luxS* strain. Small RNAs have been implicated in regulating pathways involved in QS.[49] To investigate the effect of a *luxS* mutation on small RNAs in *B. anthracis,* we utilized an Affymetrix custom genome tiled array. This platform permitted us to investigate the transcriptional activity of small and antisense RNAs. Analysis of pXO1 revealed several regions on the virulence plasmid demonstrating differential transcriptional activity in intergenic regions (**Fig. 5**). The intergenic region between locus BXA0122 and BXA0124 had substantial transcriptional activity. Furthermore, a comparison of the 34F$_2$Δ*luxS* strain with the wildtype demonstrated a lower transcriptional profile, suggesting that *luxS*/AI-2 may play a role in regulating the transcriptional activity of small RNAs in *B. anthracis*. However, to better understand the regulatory network of *luxS*/AI-2-mediated QS, additional experiments will be necessary.

Figure 4. Analysis of respiratory nitrate genes in strain 34F$_2$Δ*luxS* compared to strain 34F$_2$ and strain 34F$_2$ exposed to 20 μg/ml of fur-2 using LEM. Time points (left-most 4 columns) and sample (exposure to fur-2 for one hour; right-most column) are indicated at the top of each column. Arrows indicate the direction of gene orientation. The color scale indicates the log$_2$ changes in expression, according to the scale shown above. Locus ID based on *B. anthracis* strain Ames.

Discussion

In this study, we were able to complement the *luxS*/AI-2 deficiency in the 34F$_2$Δ*luxS* mutant. First, we assessed whether insertion of the *luxS* ORF plus its putative promoter into the *plcR* locus, creating 34F$_2$Δ*luxS*:comp strain, would restore *luxS*/AI-2 activity. Cell-free medium collected from the 34F$_2$Δ*luxS*:comp strain was able to fully stimulate luminescence in the *V. harveyi* reporter strain (**Fig. 1**), indicating that the *B. anthracis* 34F$_2$Δ*luxS*:comp strain produces AI-2 or an AI-2-like molecule,
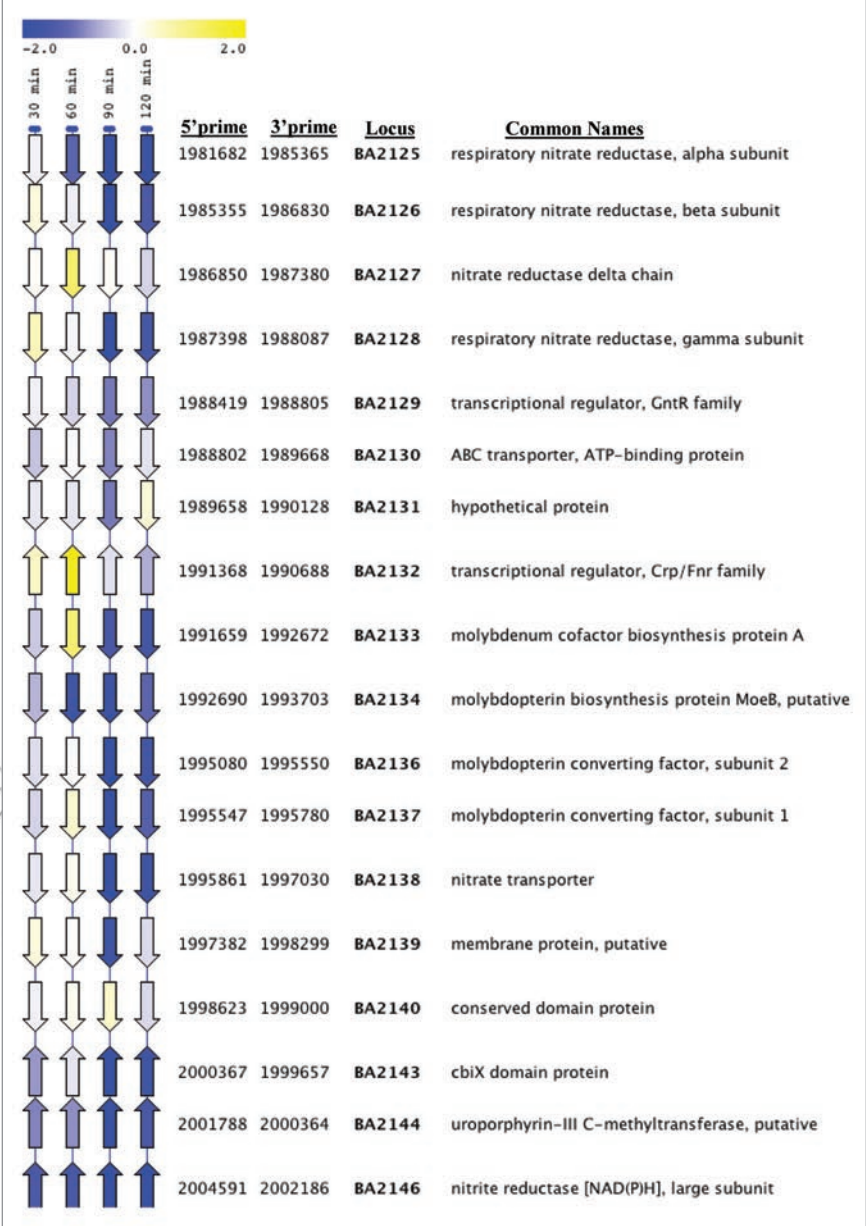
likely similar in structure to AI-2 from *V. harveyi*. Serial dilutions of CFM collected from the 34F$_2$Δ*luxS*:comp strain were able to stimulate luminescence in the *V. harveyi* strain to a similar extent as the wild-type 34F$_2$ strain, providing strong evidence that the strain is fully complemented for AI-2 activity. The growth defect observed in the *B. anthracis* Δ*luxS* strain suggests that *luxS* is involved in regulating *B. anthracis* growth. That the growth of *B. anthracis* strain Δ*luxS*:comp was restored to wildtype levels (**Fig. 2**) provides direct evidence that *luxS* is in fact involved in regulating *B. anthracis* growth. Regulation of growth by *luxS*
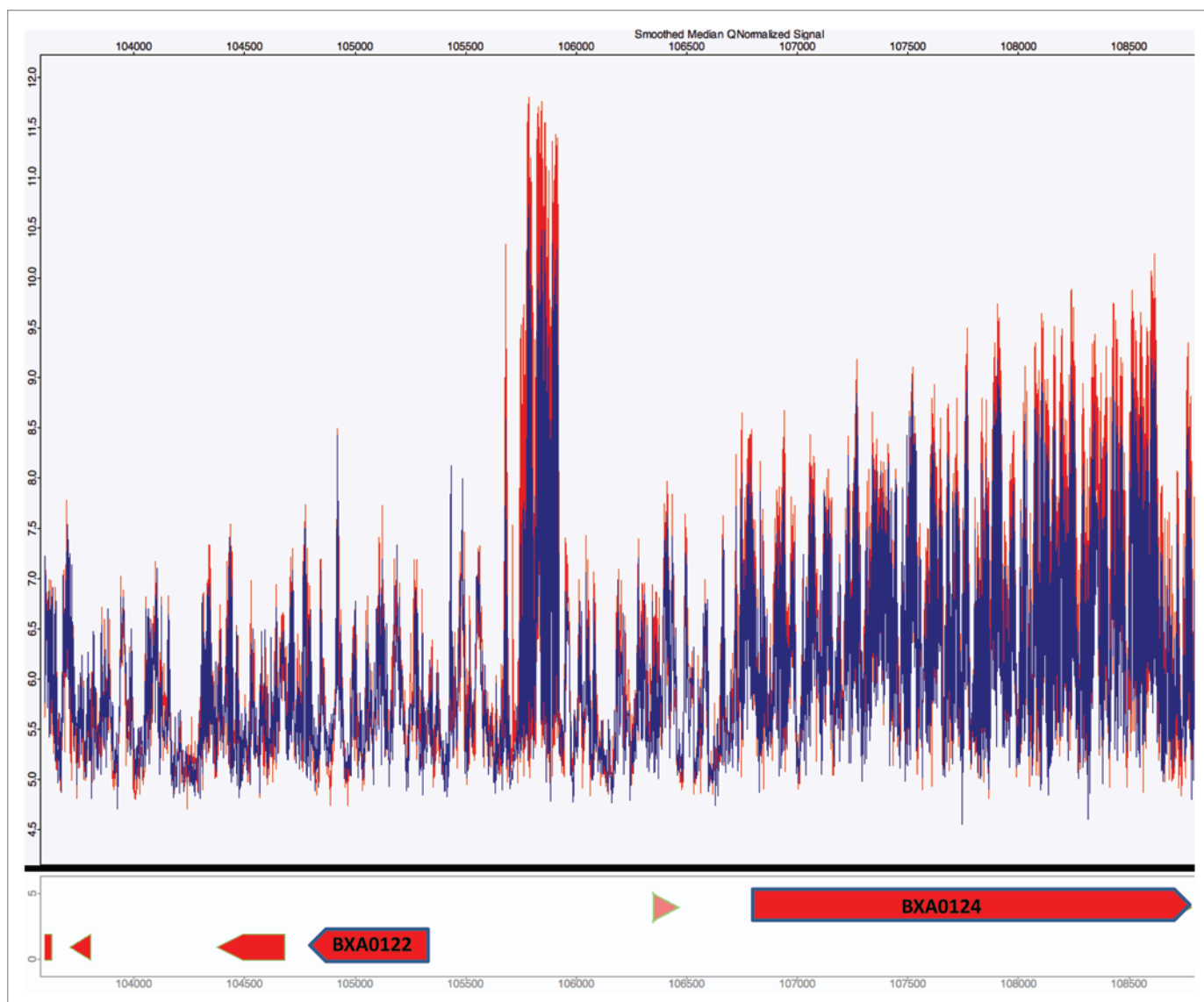
Figure 5. Analysis of small non-coding RNA of strain 34F$_2$Δ*luxS* compared to strain 34F$_2$ using an Affymetrix tiled array. A select region (between BXA0122 and BXA0124) based on pXO1 from *B. anthracis* strain A2012, demonstrating transcriptional activity in intergenic regions. Red indicates the transcriptional activity of the parental strain and blue represents strain 34F$_2$Δ*luxS*.

has been observed in *Streptococcus pyogenes*.[50] In total, these data demonstrate that the altered phenotypes in the Δ*luxS* strain are due to *luxS* disruption and not to other undefined coincident mutations.

To better understand the role of *luxS*/AI-2-mediated QS in regulating *B. anthracis* gene expression and growth regulation, we utilized microarray analysis. Our use of microarrays permitted us to identify a number of genes potentially regulated by the *luxS*/AI-2 QS system, but which in total represent <1% of those in the *B. anthracis* genome. Downregulation in the Δ*luxS* strain of key virulence genes *pagA*, *pagR*, *lef* and *cya*, is notable. Inhibition of nitrate metabolism might explain the growth defect present in the 34F$_2$*luxS* strain. The observed inhibition of the plasmid-encoded toxin gene expression may or may not be direct; AI-2 can modulate the expression of *Vibrio cholerae*

toxins in concert with small RNAs (sRNA).[44] Furthermore, recent data has demonstrated that small RNAs play a critical role in regulating virulence and sporulation in *V. cholerae* and *B. subtilis*, respectively.[51-54] One potential mechanism for *luxS*/AI-2-mediated quorum-sensing modulation of *B. anthracis* toxin expression is through the regulation of sRNAs. Detection of AI-2 by bacterial cells could potentially up or downmodulate regulatory small RNAs, leading to differential expression of the *B. anthracis* toxins.

To further understand the mechanisms by which *B. anthracis* utilizes the *luxS*/AI-2-mediated QS system to regulate growth-phase-dependent gene expression, we studied halogenated furanones, known inhibitors of QS.[30-36,55] Furanone-1 [(5Z)-4-bromo-5-(bromomethylene)-3-butyl-2(5H)-furanone] has been shown to inhibit >70% of the AI-2 regulated genes in *E. coli*,

without affecting bacterial growth rate.[31] We recently showed that halogenated furanones inhibit *B. anthracis* growth in a dose-dependent manner, and can inhibit the expression of *lacZ* when fused to the promoters of the toxin components.[30] The microarray analyses now reveal that treatment of cells with furanone (fur-2) results in inhibition of the transcription of virulence genes *lef* and *cya* on pXO1, and respiratory nitrate systems (Open reading frames BA2125-28, BA2133-38 and BA2142-46). Upstream sequence analysis of each potential operon revealed a conserved promoter motif, suggesting coordinate regulation of these operons (**Suppl. Table 1**). However this motif was not found upstream of *atxA* or other virulence genes. These data indicate that fur-2 inhibits *B. anthracis* virulence gene expression and may lead to the development of a novel therapeutic agent against anthrax infections. In *Pseudomonas aeruginosa*, respiratory nitrate regulation has been implicated to be QS-dependent.[56]

We conclude that *B. anthracis* utilizes *luxS* to regulate AI-2-dependent QS and bacterial growth; with specific regulation of expression of the S-layer protein EA1, respiratory nitrate systems and potentially, the lethal and edema toxins. We do recognize the limitation of our study working with an attenuated strain lacking pXO2. The experimentation performed in a pXO2-strain done for reasons concerning biosafety, however it would be fascinating to know what impact the pX02-background might have on the gene expression patterns measure. We further conclude that the study of halogenated furanones may be used to guide development of novel inhibitors of *B. anthracis* virulence gene expression, as well as novel treatments for anthrax. Finally, identification of small RNAs on pXO1 suggests a novel mechanism for the regulation of virulence gene expression in *B. anthracis*. Further interrogating these small RNAs may illuminate greater understanding on how the toxins are expressed, since no *atxA* binding motif has ever been identified.

Materials and Methods

Bacterial strains and culture conditions. *B. anthracis* strains 34F$_2$ (Colorado Serum Company, Denver, CO), 34F$_2\Delta luxS$ and 34F$_2\Delta luxS$:comp were routinely grown in Brain Heart Infusion broth (BHI) or BHI with 0.8% sodium bicarbonate at 37°C. *Escherichia coli* strain DH5α was routinely grown in Luria-Bertani broth (LB) at 37°C. Ampicillin (50 μg/ml) was added for cultivation of DH5α strains harboring recombinant plasmids. *V. harveyi* strain BB170, kindly provided by Bonnie Bassler (Princeton University, Princeton, NJ), was routinely grown in Auto-inducer Bioassay medium (AB) at 30°C.[57,58]

Generation of cell-free culture medium and *V. harveyi* bioassays. *B. anthracis* strains were grown overnight with aeration at 37°C. Cell-free conditioned culture medium (CFM) was prepared by centrifugation of cultures at 4,000 rpm (Eppendorf Centrifuge 5810R) and passing the medium through a 0.2 μm pore-size MILLIPORE syringe filters (Carrigwohill Company, Cork, Ireland). CFM preparations were stored at -20°C until used. CFM from *V. harveyi* strain BB170 was prepared in the same manner, except that cultures were grown at 30°C. *V. harveyi*

Table 1. Oligonucleotide primers used in this study

Primer designation	Nucleotide sequence (5′ → 3′)[a]
P1F	TTTGAACGTGCGATGAAAG
P2R	GATTGTGGAACTGATGTAACAG
P3F	GCGGATCCATTGAAGAAACTGCTGAAGCTC
P4R	GCGGATCCAGGAATAGATGTATATCAGAAC
P5F	CGTTAAAGCCTGATGTAAGCA
P6R	GGTTACGTGGTTGCTTAC
P9F	GCGGATCCTTAAAGTATTATAGCACGACTG
P10R	GCTCTACAAATATCCAGTGTCGAAACGTC
P11F	GCGGTACCTTTGAACGTGCGATGAAAG
P12R	GCGGTACCGATTGTGGAACTGATGTAACAG
BAluxSF	ATGCATCAGTAGAAAGCTTTG
BAluxSR	TTATCCAAATACTTTCTCAAGTTC

[a]Restriction sites underlined; *Bam*HI (GGATCC) and *Kpn*I (GGTACC).

bioluminescence assays were performed essentially as previously described.[37] Briefly, *V. harveyi* strain BB170 was grown at 30°C with aeration for 16 h, cultures were diluted 1:10,000 in fresh AB broth, and then 10% CFM or dilutions thereof from the bacterial cultures to be tested was added. Aliquots of 1.0-ml were taken 5 h after CFM was added, and bioluminescence measured, expressed as relative light units (RLU), using a luminometer.

Construction of a *B. anthracis* Δ*luxS*: complement strain. To complement the *luxS* deletion in *B. anthracis* strain 34F$_2\Delta luxS$, the *plcR* operon, which encodes a pleiotropic regulator of hemolysins and phospholipases in *Bacillus cereus*, was selected as the site for integration of the *luxS* complementation cassette. In wild-type *B. anthracis* strains, *plcR* contains a nonsense mutation making it naturally inactive and thus a neutral spot for an in trans complementation locus.[59] The *luxS* ORF including its putative promoter were cloned into the *plcR* ORF. PCR was used to amplify a 3 kb fragment from the *plcR* locus, including 1.05 kb upstream and 1.1 kb downstream of the *plcR* ORF using primers P1 and P2 (**Table 1**). The PCR-amplified product was purified using a PCR purification kit (Qiagen, Valencia, CA), and subsequently cloned into pGEM-T easy. A plasmid with the correct insert and orientation was designated pMJ601. pMJ601 was modified by inverse PCR to add *Bam*HI sites (primers P3 and P4; **Table 1**) in the middle of the cloned insert for insertion of the *luxS* complementation cassette. The *luxS* complementation cassette was created by using purified chromosomal DNA of *B. anthracis* strain 34F$_2$. *B. anthracis luxS* was cloned using primers P9 and P10 to generate a 715-bp fragment including the putative *luxS* promoter. Downstream of the *luxS* ORF an erythromycin resistance cassette (Erm^R) was inserted into the XbaI/BamHI site by restriction digest to enable selection for plasmid integration. Finally, primers P11 and P12 (**Table 1**) were used to clone the *plcR* region containing the *luxS*/Erm^R complementation cassette into *B. anthracis* shuttle vector pUTE29 that confers Tet^R. A plasmid with the correct insert was designated pMJ602ET. Purified pMJ602ET from SCS110 was electroporated into *B. anthracis* strain 34F$_2$:Δ*luxS* and colonies selected

Table 2. *B. anthracis* chromosomal genes upregulated in the 34F$_2$Δ*luxS* strain as determined by microarray analysis, sorted by locus

Locus[c]	Gene Name[b]	30 min[a]	60 min	90 min	120 min
BA0194	oligopeptide ABC transporter, oligopeptide-binding protein	1.42	5.03	4.44	7.67
BA0369	methyl-accepting chemotaxis protein	6.15	11.47	6.68	6.28
BA0558	methyl-accepting chemotaxis protein	12.47	11.47	11.00	9.85
BA0575	methyl-accepting chemotaxis protein	4.86	7.16	6.45	8.51
BA0677	phospholipase C (plc)	4.14	7.06	5.28	6.54
BA0682	hypothetical protein	3.46	5.70	7.06	6.36
BA0796	conserved hypothetical protein	2.20	5.39	6.82	16.56
BA2025	hypothetical protein	9.32	14.22	10.85	12.73
BA2114	RNA polymerase sigma-70 factor, ECF subfamily	1.17	3.61	6.82	12.21
BA2115	hypothetical protein	1.68	3.48	7.84	9.99
BA2363	transcriptional regulator, ArsR family	3.78	11.63	12.38	7.67
BA2606	hypothetical protein	7.52	11.63	7.94	6.41
BA2732	RNA polymerase sigma factor SigX, putative	1.35	2.77	15.67	64.00
BA3029	succinylornithine transaminase, putative	1.23	4.89	7.41	7.78
BA3034	hypothetical protein	1.55	5.06	4.23	8.22
BA3114	membrane protein, putative	13.45	10.78	7.36	11.24
BA3305	transcriptional regulator, ArsR family	3.76	7.67	5.06	10.34
BA3405	ABC transporter, permease protein	1.28	1.83	8.57	11.63
BA3406	ABC transporter, ATP-binding protein	0.71	2.46	6.77	18.13
BA3407	hypothetical protein	1.08	2.22	7.11	8.28
BA4264	nitroreductase family protein	1.52	2.81	3.97	7.16
BA5481	conserved domain protein	7.31	14.03	4.89	7.26
BA5628	iron compound ABC transporter	1.85	4.11	3.76	7.01

[a]Numbers represent fold change over the 120 min time course of the experiments; [b]Functional annotations were obtained from the *B. anthracis* complete genome sequence (www.jcvi.org); [c]Locus based on Ames strain of *B. anthracis*.

for erythromycin resistance. Transformants were initially picked on medium containing 5 μg/ml of erythromycin, and then subcultured twice daily in the absence of antibiotics at 37° with aeration, for 15 days. Individual colonies were subsequently screened to identify clones that were both Erm[R] and Tet[S]. This would suggest loss of pMJ602ET and incorporation of the modified *plcR* allele into the chromosome. For clones with the appropriate antibiotic phenotype, the correct insertion was confirmed by PCR using primers luxSF/P6 and luxSR/P5 (**Table 1**).

RNA isolation for microarray analysis. *B. anthracis* RNA was isolated from bacterial cultures grown to mid-log in BHI media with or without sodium bicarbonate, RNAprotect (Qiagen) was directly added to the growth media at a concentration of 2:1 (volume of RNAprotect to bacterial culture). RNA was isolated from bacterial cultures grown in the presence of or the absence of furanone-2 (fur-2; 3-butyl-5-(dibromomethylene)-2-(5*H*)-furanone), as stated above. Cells treated with RNAprotect were pelleted and stored at -80°C until RNA extraction, using the Ambion mirVana RNA kit (Austin, TX) in combination with the Barocycler (Pressure BioSciences, South Easton, MA). RNA quantity and quality was assessed by measuring total RNA using a nanodrop 1000 spectrophotometer (Thermo Scientific) and visualizing RNA on an agarose gel. Purified RNA was stored at -80°C.

Generation of probes for microarray experiments. DNA probes for microarray experiments were generated by adding 2 μg of total RNA in a mixture containing 6 μg of random hexamers (Invitrogen), 0.01 M dithiothreitol, an aminoallyl-deoxynucleoside triphosphate mixture containing 25 mM each dATP, dCTP and dGTP, 15 mM dTTP, and 10 mM amino-allyl-dUTP (aa-dUTP) (Sigma), reaction buffer, and 400 units of SuperScript III reverse transcriptase (Invitrogen) at 42°C overnight. The RNA template then was hydrolyzed by adding NaOH and EDTA to a final concentration of 0.2 and 0.1 M, respectively, and incubating at 65°C for 15 min. Unincorporated aa-dUTP was removed with a Minelute column (Qiagen). The probe was eluted with a phosphate elution buffer (4 mM KPO$_4$, pH 8.5, in ultrapure water), dried and resuspended in 0.1 M sodium carbonate buffer (pH 9.0). To couple the amino-allyl cDNA with fluorescent labels, normal human serum-Cy3 or normal human serum-Cy5 (Amersham) was added at room temperature for 1 h. Uncoupled label was removed using the Qiagen Minelute column (Valencia, CA) (intranet.jtc.jcvsf.org/sops/M007.pdf).

Microarray hybridization, scanning, image analysis, normalization and analysis. Aminosilane-coated slides printed with a set of 15,552 *B. anthracis* open reading frame sequences (www.jcvi.org) were prehybridized in 5x SSC (1x SSC is 0.15 M NaCl plus 0.015 M sodium citrate) (Invitrogen), 0.1% sodium dodecyl

Table 3. *B. anthracis* chromosomal genes downregulated in the 34F₂Δ*luxS* strain as determined by microarray analysis, sorted by locus

Locus[c]	Gene name[b]	30 min[a]	60 min	90 min	120 min
BA0238	hypothetical protein	-3.41	-29.65	-5.78	-15.78
BA0239	hypothetical protein	-3.86	-22.16	-5.86	-19.29
BA0240	4-hydroxyphenylpyruvate dioxygenase (*hppD*)	NaN	-11.63	-9.51	-6.41
BA0509	formate acetyltransferase (*pfl*)	-33.13	-125.37	-56.89	-35.51
BA0510	pyruvate formate-lyase-activating enzyme (*pflA*)	-1.26	-23.26	-36.00	-21.71
BA0668	ribose ABC transporter, permease protein (*rbsC*)	-1.42	-14.42	-12.91	-7.94
BA0669	ribose ABC transporter, ribose-binding protein (*rbsB*)	-1.58	-15.89	-11.88	-6.96
BA0887	S-layer protein EA1 (*eag*)	-7.26	-25.63	-46.85	-3.97
BA1086	sugar-binding transcriptional regulator, LacI family	-3.14	-19.29	-11.08	-4.20
BA2125	respiratory nitrate reductase, alpha subunit (*narG*)	-6.68	-4.20	-52.71	-42.22
BA2126	respiratory nitrate reductase, beta subunit (*narH*)	-1.13	-3.18	-29.24	-17.39
BA2128	respiratory nitrate reductase, gamma subunit (*narI*)	-1.25	-3.12	-38.59	-18.13
BA2133	molybdenum cofactor biosynthesis protein A (*narA-1*)	-1.84	-6.36	-45.25	-14.83
BA2134	molybdopterin biosynthesis protein MoeB, putative	-1.07	-5.06	-103.97	-13.55
BA2135	molybdopterin biosynthesis protein MoeA (*moeA-1*)	-1.12	-2.19	-35.26	-13.64
BA2136	molybdopterin converting factor, subunit 2 (*moaE-1*)	-1.13	-2.95	-48.84	-20.53
BA2137	molybdopterin converting factor, subunit 1 (*moaD-1*)	-1.36	-1.91	-22.78	-29.86
BA2138	nitrate transporter (*narK*)	-1.24	-1.92	-37.53	-21.11
BA2146	nitrite reductase [NAD(P)H], large subunit (*nirB*)	-1.33	-76.11	-60.97	-210.84
BA2267	alcohol dehydrogenase, zinc-containing	-3.61	-12.91	-6.45	-9.19
BA2295	acetate CoA-transferase, subunit A (*atoD*)	-1.01	NaN	-8.11	-22.16
BA2350	carboxyvinyl-carboxyphosphonate phosphorylmutase (*yqiQ*)	-1.52	-5.24	-12.13	-19.16
BA2547	acyl-CoA dehydrogenase	-2.01	-13.36	-19.70	-10.48
BA2548	acetyl-CoA carboxylase, biotin carboxylase, putative	-1.66	-7.06	-17.27	-9.99
BA2552	carboxyl transferase domain protein	-1.24	-16.45	-11.39	-10.27
BA3479	transcriptional regulator, ArsR family	-36.00	-44.94	-37.27	-136.24
BA3481	hypothetical protein	-38.85	-315.17	-137.19	-69.55
BA3482	conserved hypothetical protein	-32.67	-36.00	-64.45	-140.07
BA3483	conserved hypothetical protein	-30.48	-67.18	-53.82	-219.79
BA3663	anaerobic ribonucleoside-triphosphate reductase	NaN	-14.03	-4.66	-9.92
BA5047	autoinducer-2 production protein LuxS (*luxS*)	-14.72	-28.84	-29.86	-494.56
BA5696	superoxide dismutase, Mn (*sodA-2*)	-1.77	-7.62	-14.62	-7.11

[a]Numbers represent fold change over the 120 min time course of the experiments; [b]Functional annotations were obtained from the *B. anthracis* complete genome sequence (www.jcvi.org); [c]Locus based on Ames strain of *B. anthracis*; [d]NaN indicates a miss data point.

sulfate and 1% bovine serum albumin at 42°C for 60 min. The slides then were washed at room temperature with distilled water, dipped in isopropanol and allowed to dry. Equal volumes of the appropriate Cy3- and Cy5-labeled probes were combined, dried and then resuspended in a solution of 40% formamide, 5x SSC and 0.1% sodium dodecyl sulfate. Resuspended probes were heated to 95°C prior to hybridization. The probe mixture then was added to the microarray slide and allowed to hybridize overnight at 42°C. Hybridized slides were washed sequentially in solutions of 1x SSC-0.2% SDS, 0.1x SSC-0.2% SDS and 0.1x SSC at room temperature, then dried in air and scanned with an Axon GenePix 4000 scanner (intranet.jtc.jcvsf.org/sops/M008.pdf). All wash buffers were supplemented with 1-ml of 0.1 M DTT per liter of wash buffer. Individual TIFF images from each

channel were analyzed with TIGR Spotfinder (available at (pfgrc.jcvi.org/index.php/bioinformatics.html). Microarray data were normalized by LOWESS normalization and with in-slide replicate analysis using TM4 software MIDAS (available at (pfgrc.jcvi.org/index.php/bioinformatics.html).[38,60] We selected genes in which comparison of wild-type cells exposed to diluent alone and cells exposed to 20 μg/ml of fur-2 yielded log₂ value |≥1.5| in all samples. We also selected genes that had a log₂ value |≥1.5| in all samples, comparing wild-type cells to Δ*luxS* cells. Genes with a log₂ value |≤1.5| but a log₂ value |≥1| were selected if the gene appeared in the middle of an operon.

Analysis of upstream promoter motifs. A selected set of genes that appeared to be co-regulated in the linear expression map were analyzed to discover motifs in upstream areas that may identify

Table 4. Select genes downregulated on pXO1 in *B. anthracis* 34F$_2$Δ*luxS* as determined by microarray analysis, sorted by locus

Locus[c]	Gene name[b]	30 min[a]	60 min	90 min	120 min
BXA0142	**calmodulin-sensitive adenylate cyclase (*cya*)**	**1.03**	**-2.00**	**-3.46**	**-4.69**
BXA0146	**transcriptional activator AtxA (*atxA*)**	**-1.34**	**-1.16**	**-1.25**	**-1.83**
BXA0164	**protective antigen (*pagA*)**	**-1.02**	**-1.53**	**-7.21**	**-26.17**
BXA0165	hypothetical protein	1.21	-1.74	-7.52	-20.97
BXA0166	**transcriptional repressor PagR (*pagR*)**	**-1.13**	**-2.13**	**-6.11**	**-13.36**
BXA0167	hypothetical protein	1.36	-1.39	-5.70	-10.27
BXA0168	hypothetical protein	-1.20	-1.13	-2.46	-2.62
BXA0169	hypothetical protein	-1.23	-1.20	-2.10	-2.89
BXA0170	hypothetical protein	-1.24	1.16	-1.71	-4.23
BXA0171	ribonuclease domain protein	-1.59	-1.49	-2.99	-7.62
BXA0172	**lethal factor (*lef*)**	**-1.02**	**1.05**	**-2.71**	**-4.92**

[a]Numbers represent fold change over the 120 min time course of the experiments; Bolded genes indicate genes involved in *B. anthracis* toxin production or its regulation; [b]Functional annotations were obtained from the *B. anthracis* complete genome sequence (www.jcvi.org); [c]Locus based on Ames strain of *B. anthracis*.

Table 5. Select virulence genes downregulated on pXO1 in 34F$_2$Δ*luxS* compared to 34F$_2$*luxS*:comp

Locus[c]	Gene name[b]	120 min[a]
BXA0124	S-layer protein	-5.16
BXA0142	**calmodulin-sensitive adenylate cyclase**	**-3.97**
BXA0146	**transcriptional activator AtxA**	**-2.9**
BXA0164	**protective antigen**	**-13.78**
BXA0165	hypothetical protein	-16.83
BXA0166	**transcriptional repressor PagR**	**-14.66**
BXA0172	**lethal factor**	**-4.32**

[a]Numbers represent fold change over; Bolded genes indicate genes involved in *B. anthracis* toxin production or its regulation; [b]Functional annotations were obtained from the *B. anthracis* complete genome sequence (www.jcvi.org); [c]Locus based on *B. anthracis* strain A2012.

Table 6. Select *B. anthracis* genes on pXO1 downregulated by fur-2

Locus[c]	Gene name[b]	Symbol	120 min[a]
BXA0124	S-layer protein		-16.63
BXA0142	calmodulin-sensitive adenylate cyclase	*cyaA*	-1.41
BXA0146	transcriptional activator AtxA	*atxA*	-1.34
BXA0164	protective antigen	*pagA*	-13.48
BXA0166	transcriptional repressor PagR	*pagR*	-5.81
BXA0172	lethal factor	*lef*	-2.03

[a]Numbers represent fold change; [b]Functional annotations were obtained from the *B. anthracis* complete genome sequence (www.jcvi.org); [c]Locus based on *B. anthracis* strain A2012.

common transcription factor binding sites. For motif discovery analysis, 200 base sequences upstream of each gene in the genome were collected. These upstream sequences were truncated when necessary to exclude sequences that crossed a neighboring gene boundary. Upstream sequences less than 30 bases were excluded. If the gene was transcribed on the minus strand, the reverse complement of the upstream region was analyzed. Motif finding was performed using the discriminative motif finding tool, DEME.[61] DEME requires two input sequence lists; one input corresponds to upstream areas believed to possibly contain a shared motif and the other set consists of upstream sequences of genes that are thought to not contain the motif within the positive group. The algorithm attempts to find a motif that best separates the positive group of upstream sequences corresponding to the co-regulated gene

set from the negative set, representing all other upstream sequences in the genome. A 15 base window was used and the reverse complement of each upstream section also was analyzed. DEME reports a consensus motif and upstream sequence matches for each positive *and* negative sequence. NCBI refseq was the source for the whole genome sequence file and the coordinate file (ptt file) used to extract upstream sequences.

Analysis of small RNAs in *B. anthracis* 34F₂Δ*luxS* strain. Cells were grown to early log phase and pellets collected at 30, 60, 90 and 120 minutes. Total RNA was extracted from cell pellets previously treated with RNAprotect (Qiagen), and the extracted RNAs were treated with Turbo DNA-free DNase (Ambion), then converted to cDNA and labeled according to the Affymetrix protocol. Labeled probes were hybridized onto the Affymetrix platform and incubated overnight in an Affymetrix oven. Chips were washed, scanned and .CEL files were imported into genomeMTV (www.genomeMTV.org) for analysis. Data were normalized by the genomeMTV software, based on quantum normalization. Analysis of pXO1 using the sliding window of genomeMTV

permitted us to visually scan the virulence plasmid and inspect for intergenic transcriptional activity.

Note

Supplementary materials can be found at:
www.landesbioscience.com/supplement/JonesVIRU1-2-Sup1.xls
www.landesbioscience.com/supplement/JonesVIRU1-2-Sup2.pdf

References

1. Dutz W, Kohout E. Anthrax. Pathol Annu 1971; 6:209-48.
2. Hambleton P, Carman JA, Melling J. Anthrax: the disease in relation to vaccines. Vaccine 1984; 2:125-32.
3. Turnbull PC. Anthrax vaccines: past, present and future. Vaccine 1991; 9:533-9.
4. Ullmann A, Mock M. A particular class of virulence factors: calmodulin-activated bacterial adenylate cyclases. Zentralbl Bakteriol 1994; 281:284-95.
5. Makino S, Uchida I. The pathogenesis of *Bacillus anthracis*. Nippon Saikingaku Zasshi 1996; 51:833-40.
6. Hanna PC, Ireland JA. Understanding *Bacillus anthracis* pathogenesis. Trends Microbiol 1999; 7:180-2.
7. Brossier F, Mock M. Toxins of *Bacillus anthracis*. Toxicon 2001; 39:1747-55.
8. Mock M, Fouet A. Anthrax. Annu Rev Microbiol 2001; 55:647-71.
9. Koehler TM. *Bacillus anthracis* genetics and virulence gene regulation. Curr Top Microbiol Immunol 2002; 271:143-64.
10. Mock M, Mignot T. Anthrax toxins and the host: a story of intimacy. Cell Microbiol 2003; 5:15-23.
11. Ahuja N, Kumar P, Bhatnagar R. The adenylate cyclase toxins. Crit Rev Microbiol 2004; 30:187-96.
12. Moayeri M, Leppla SH. The roles of anthrax toxin in pathogenesis. Curr Opin Microbiol 2004; 7:19-24.
13. Mock M, Ullmann A. Calmodulin-activated bacterial adenylate cyclases as virulence factors. Trends Microbiol 1993; 1:187-92.
14. Brossier F, Guidi-Rontani C, Mock M. Anthrax toxins. C R Seances Soc Biol Fil 1998; 192:437-44.
15. Hanna P. Anthrax pathogenesis and host response. Curr Top Microbiol Immunol 1998; 225:13-35.
16. Little SF, Ivins BE. Molecular pathogenesis of *Bacillus anthracis* infection. Microbes Infect 1999; 1:131-9.
17. Liu S, Schubert RL, Bugge TH, Leppla SH. Anthrax toxin: structures, functions and tumour targeting. Expert Opin Biol Ther 2003; 3:843-53.
18. Abrami L, Reig N, van der Goot FG. Anthrax toxin: the long and winding road that leads to the kill. Trends Microbiol 2005; 13:72-8.
19. Sirard JC, Mock M, Fouet A. The three *Bacillus anthracis* toxin genes are coordinately regulated by bicarbonate and temperature. J Bacteriol 1994; 176:5188-92.
20. Gray KM. Intercellular communication and group behavior in bacteria. Trends Microbiol 1997; 5:184-8.

21. Morrison DA. Streptococcal competence for genetic transformation: regulation by peptide pheromones. Microb Drug Resist 1997; 3:27-37.
22. Hardman AM, Stewart GS, Williams P. Quorum sensing and the cell-cell communication dependent regulation of gene expression in pathogenic and non-pathogenic bacteria. Antonie Van Leeuwenhoek 1998; 74:199-210.
23. Bassler BL. How bacteria talk to each other: regulation of gene expression by quorum sensing. Curr Opin Microbiol 1999; 2:582-7.
24. Miller MB, Bassler BL. Quorum sensing in bacteria. Annu Rev Microbiol 2001; 55:165-99.
25. Bassler BL. Small talk. Cell-to-cell communication in bacteria. Cell 2002; 109:421-4.
26. Manefield M, Welch M, Givskov M, Salmond GP, Kjelleberg S. Halogenated furanones from the red alga, *Delisea pulchra*, inhibit carbapenem antibiotic synthesis and exoenzyme virulence factor production in the phytopathogen *Erwinia carotovora*. FEMS Microbiol Lett 2001; 205:131-8.
27. Hentzer M, Givskov M. Pharmacological inhibition of quorum sensing for the treatment of chronic bacterial infections. J Clin Invest 2003; 112:1300-7.
28. Hentzer M, Wu H, Andersen JB, Riedel K, Rasmussen TB, Bagge N, et al. Attenuation of *Pseudomonas aeruginosa* virulence by quorum sensing inhibitors. EMBO J 2003; 22:3803-15.
29. Smith KM, Bu Y, Suga H. Induction and inhibition of *Pseudomonas aeruginosa* quorum sensing by synthetic autoinducer analogs. Chem Biol 2003; 10:81-9.
30. Jones MB, Jani R, Ren D, Wood TK, Blaser MJ. Inhibition of *Bacillus anthracis* Growth and Virulence-Gene Expression by Inhibitors of Quorum-Sensing. J Infect Dis 2005; 191:1881-8.
31. Ren D, Bedzyk LA, Ye RW, Thomas SM, Wood TK. Differential gene expression shows natural brominated furanones interfere with the autoinducer-2 bacterial signaling system of *Escherichia coli*. Biotechnol Bioeng 2004; 88:630-42.
32. Ren D, Bedzyk LA, Setlow P, England DF, Kjelleberg S, Thomas SM, et al. Differential gene expression to investigate the effect of (5Z)-4-bromo-5-(bromomethylene)-3-butyl-2(5H)-furanone on *Bacillus subtilis*. Appl Environ Microbiol 2004; 70:4941-9.

33. Ren D, Zuo R, Wood TK. Quorum-sensing antagonist (5Z)-4-bromo-5-(bromomethylene)-3-butyl-2(5H)-furanone influences siderophore biosynthesis in *Pseudomonas putida* and *Pseudomonas aeruginosa*. Appl Microbiol Biotechnol 2005; 66:689-95.
34. Ren D, Wood TK. (5Z)-4-bromo-5-(bromomethylene)-3-butyl-2(5H)-furanone reduces corrosion from *Desulfotomaculum orientis*. Environ Microbiol 2004; 6:535-40.
35. Ren D, Sims JJ, Wood TK. Inhibition of biofilm formation and swarming of *Bacillus subtilis* by (5Z)-4-bromo-5-(bromomethylene)-3-butyl-2(5H)-furanone. Lett Appl Microbiol 2002; 34:293-9.
36. Ren D, Sims JJ, Wood TK. Inhibition of biofilm formation and swarming of *Escherichia coli* by (5Z)-4-bromo-5-(bromomethylene)-3-butyl-2(5H)-furanone. Environ Microbiol 2001; 3:731-6.
37. Jones MB, Blaser MJ. Detection of a luxS-signaling molecule in *Bacillus anthracis*. Infect Immun 2003; 71:3914-9.
38. Saeed AI, Sharov V, White J, Li J, Liang W, Bhagabati N, et al. TM4: a free, open-source system for microarray data management and analysis. Biotechniques 2003; 34:374-8.
39. Morozkina EV, Zvyagilskaya RA. Nitrate reductases: structure, functions and effect of stress factors. Biochemistry (Mosc) 2007; 72:1151-60.
40. Nakano MM, Yang F, Hardin P, Zuber P. Nitrogen regulation of nasA and the nasB operon, which encode genes required for nitrate assimilation in *Bacillus subtilis*. J Bacteriol 1995; 177:573-9.
41. Ahmer BM, van Reeuwijk J, Timmers CD, Valentine PJ, Heffron F. *Salmonella typhimurium* encodes an SdiA homolog, a putative quorum sensor of the LuxR family, that regulates genes on the virulence plasmid. J Bacteriol 1998; 180:1185-93.
42. Manefield M, Harris L, Rice SA, de Nys R, Kjelleberg S. Inhibition of luminescence and virulence in the black tiger prawn (*Penaeus monodon*) pathogen *Vibrio harveyi* by intercellular signal antagonists. Appl Environ Microbiol 2000; 66:2079-84.
43. Hentzer M, Riedel K, Rasmussen TB, Heydorn A, Andersen JB, Parsek MR, et al. Inhibition of quorum sensing in *Pseudomonas aeruginosa* biofilm bacteria by a halogenated furanone compound. Microbiology 2002; 148:87-102.

44. Miller MB, Skorupski K, Lenz DH, Taylor RK, Bassler BL. Parallel quorum sensing systems converge to regulate virulence in *Vibrio cholerae*. Cell 2002; 110:303-14.

45. Whitehead NA, Byers JT, Commander P, Corbett MJ, Coulthurst SJ, Everson L, et al. The regulation of virulence in phytopathogenic Erwinia species: quorum sensing, antibiotics and ecological considerations. Antonie Van Leeuwenhoek 2002; 81:223-31.

46. Haralalka S, Nandi S, Bhadra RK. Mutation in the relA gene of *Vibrio cholerae* affects in vitro and in vivo expression of virulence factors. J Bacteriol 2003; 185:4672-82.

47. Manna AC, Cheung AL. sarU, a sarA homolog, is repressed by SarT and regulates virulence genes in *Staphylococcus aureus*. Infect Immun 2003; 71:343-53.

48. Novick RP, Jiang D. The staphylococcal saeRS system coordinates environmental signals with agr quorum sensing. Microbiology 2003; 149:2709-17.

49. Hammer BK, Bassler BL. Quorum sensing controls biofilm formation in *Vibrio cholerae*. Mol Microbiol 2003; 50:101-4.

50. Lyon WR, Madden JC, Levin JC, Stein JL, Caparon MG. Mutation of luxS affects growth and virulence factor expression in *Streptococcus pyogenes*. Mol Microbiol 2001; 42:145-57.

51. Lenz DH, Bassler BL. The small nucleoid protein Fis is involved in *Vibrio cholerae* quorum sensing. Mol Microbiol 2007; 63:859-71.

52. Lenz DH, Miller MB, Zhu J, Kulkarni RV, Bassler BL. CsrA and three redundant small RNAs regulate quorum sensing in *Vibrio cholerae*. Mol Microbiol 2005; 58:1186-202.

53. Lenz DH, Mok KC, Lilley BN, Kulkarni RV, Wingreen NS, Bassler BL. The small RNA chaperone Hfq and multiple small RNAs control quorum sensing in *Vibrio harveyi* and *Vibrio cholerae*. Cell 2004; 118:69-82.

54. Ding Y, Davis BM, Waldor MK. Hfq is essential for *Vibrio cholerae* virulence and downregulates sigma expression. Mol Microbiol 2004; 53:345-54.

55. Ren D, Zuo R, Wood TK. Quorum-sensing antagonist (5Z)-4-bromo-5-(bromomethylene)-3-butyl-2(5H)-furanone influences siderophore biosynthesis in *Pseudomonas putida* and *Pseudomonas aeruginosa*. Appl Microbiol Biotechnol 2004.

56. Toyofuku M, Nomura N, Kuno E, Tashiro Y, Nakajima T, Uchiyama H. Influence of the *Pseudomonas quinolone* signal on denitrification in *Pseudomonas aeruginosa*. J Bacteriol 2008; 190:7947-56.

57. Bassler BL, Greenberg EP, Stevens AM. Cross-species induction of luminescence in the quorum-sensing bacterium *Vibrio harveyi*. J Bacteriol 1997; 179:4043-5.

58. Bassler BL, Wright M, Silverman MR. Multiple signalling systems controlling expression of luminescence in *Vibrio harveyi*: sequence and function of genes encoding a second sensory pathway. Mol Microbiol 1994; 13:273-86.

59. Agaisse H, Gominet M, Okstad OA, Kolsto AB, Lereclus D. PlcR is a pleiotropic regulator of extracellular virulence factor gene expression in *Bacillus thuringiensis*. Mol Microbiol 1999; 32:1043-53.

60. Saeed AI, Bhagabati NK, Braisted JC, Liang W, Sharov V, Howe EA, et al. TM4 microarray software suite. Methods Enzymol 2006; 411:134-93.

61. Redhead E, Bailey TL. Discriminative motif discovery in DNA and protein sequences using the DEME algorithm. BMC Bioinformatics 2007; 8:385.